Selected Problems of Medical Image Analysis

Jiří Jan, Radovan Jiřík, Adam Filipík, Libor Kubečka, Radim Kolář

Dept. of Biomedical Engineering,

Brno University of Technology

Content of the survey:

- USCT - ultrasonic transmission computed tomography
  - reconstruction algorithms
  - transducer calibration
- Processing and analysis of bimodal retinal images
  - bimodal image registration
  - vector image based segmentation of the nerve head (optic disc)

Ultrasonic TransmissionComputed Tomography (USCT)

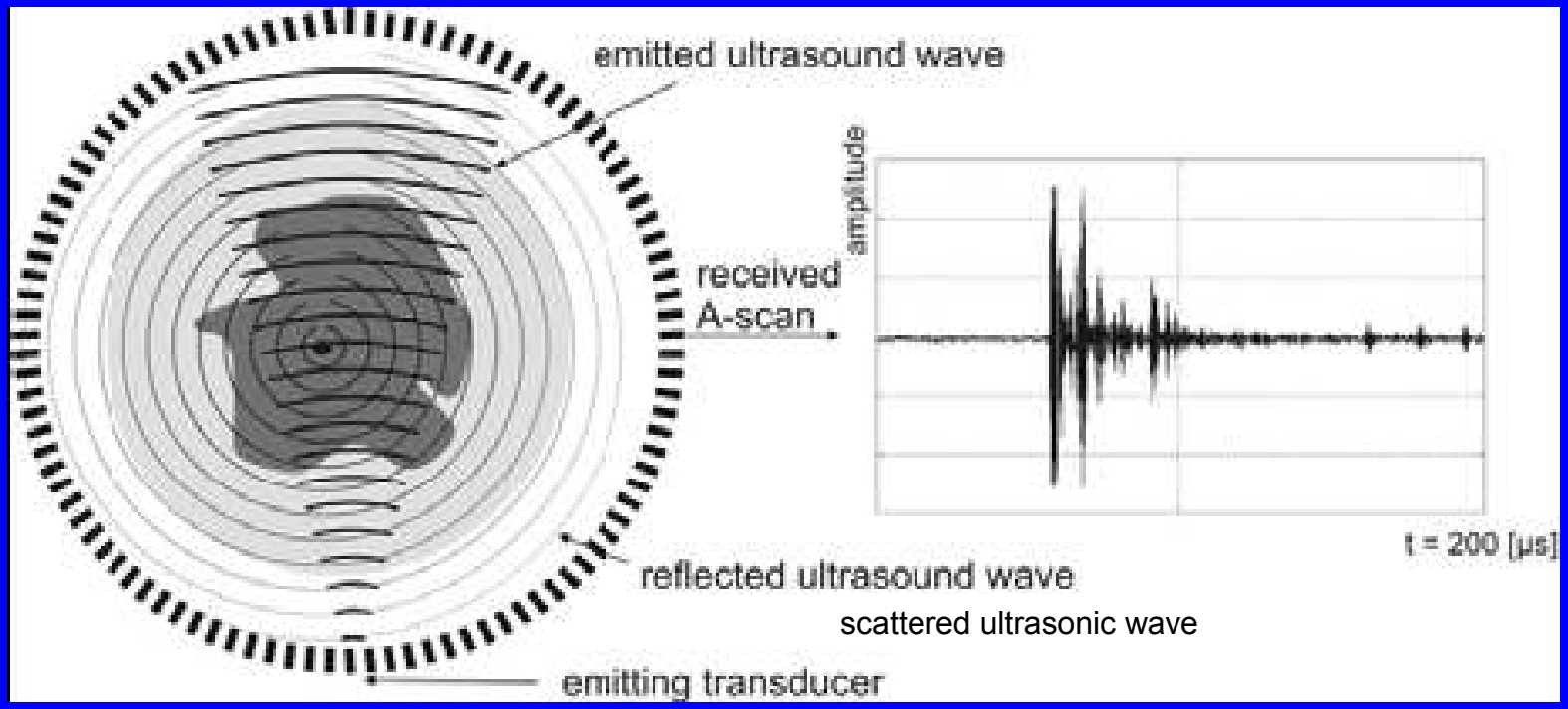

Required: reconstructed tomographic images of

- ultrasonic reflectivity
- local ultrasonic attenuation
- speed of the propagating ultrasound

Attenuation Tomography Based on Log-Spectrum Analysis

(R.Jiřík, R. Stotzka, T. Taxt - SPIE San Diego 2005)

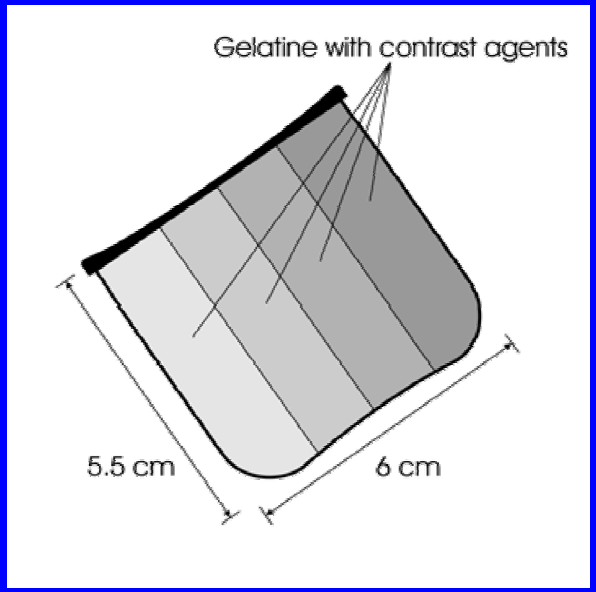

Standardní nefiltrovaná zpětná projekce

Nový alg. odhadu útlumu

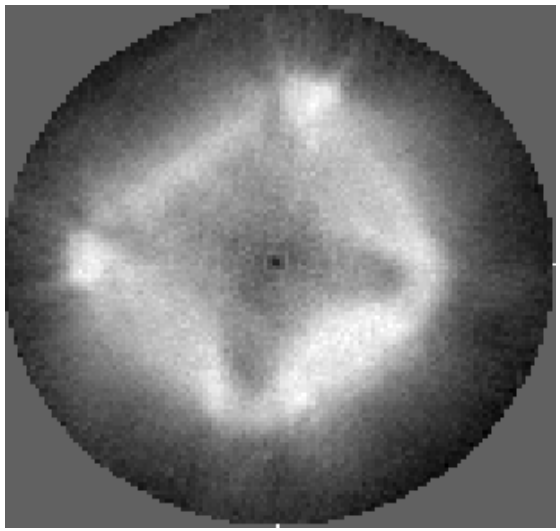

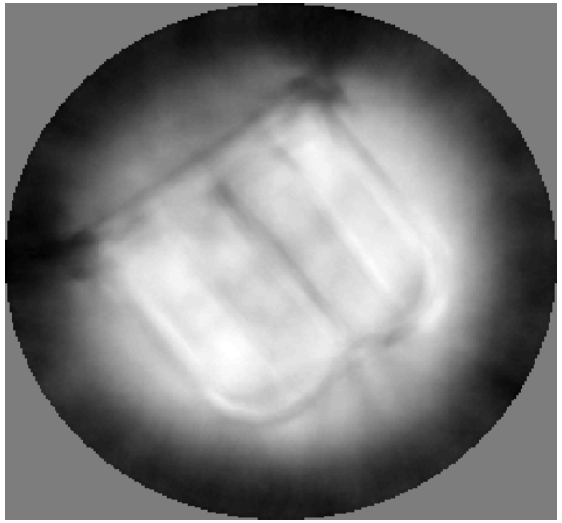

TRANSDUCER CALIBRATION IN TRANSMISSION ULTRASONIC COMPUTED TOMOGRAPHY

(A.Filipík, J.Jan, R.Jiřík – EMBEC Praha 2005)

Simplified assumptions for reconstruction:

- (semi)isotropic radiation
- equal efficiency of the transducers

More realistic (supposed to improve the reconstruction):

- real directivity characteristics (common to all transducers)
- individual efficiencies of the transducers

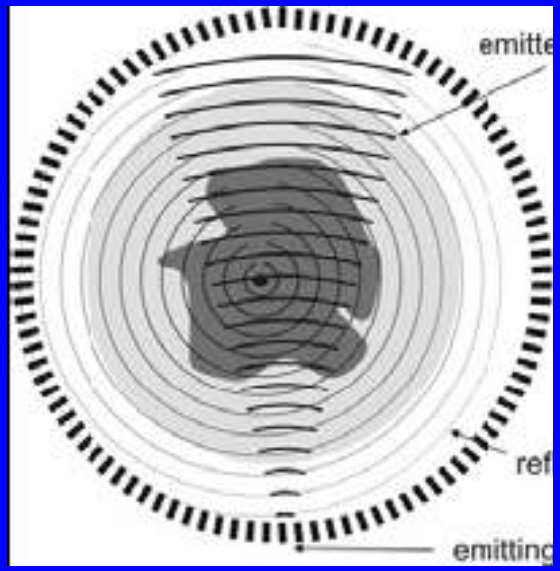

The purpose of the calibration:

to determine (via series of „empty“ measurements)

the two-dimensional angle- and frequency-dependent *radiation function*

+ the vector of individual (radiation and reception) efficiencies

Simplifying assumptions:

- linearity
- equal directivity of all transducers for both emitting and receiving
- mirror symmetry of directivity

Equation system compilation

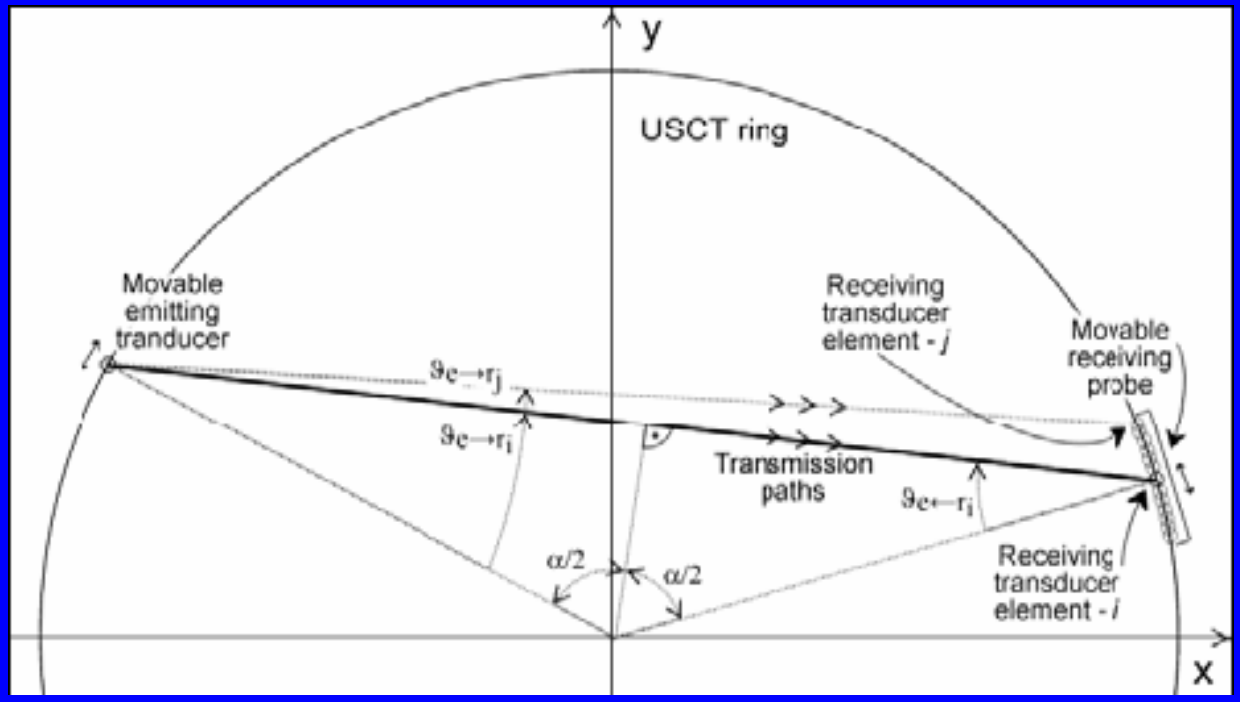

Received signal equation

$$S_{e,r}(f) \cong R_e(f, \vartheta_{e \to r}) \cdot R_r(f, \vartheta_{e \leftarrow r})$$

Log-linearised equation

$$\log\left(S_{e,r}(f)\right) = \log\left(R_e(f, \vartheta_{e \to r})\right) + \log\left(R_r(f, \vartheta_{e \leftarrow r})\right), \forall e, r$$

Available number of independent equations (given limitations of the measuring setup)

Number of unknown parameters

$$N_{r-pos} \cdot N_{r-el} \cdot N_{freq} = 91 \cdot 16 \cdot 64 = 93\,184$$

$$(1 + N_{r-el}) \cdot N_{freq} \cdot N_{ang} = (1+16) \cdot 64 \cdot (16 \cdot 91) = 1\,584\,128$$

Restricted number of equations thanks to assumptions

$$1 + N_{r-el} + N_{freq} \cdot N_{ang} = 1 + 16 + 64 \cdot (16 \cdot 46) = 47.121$$

Results of calibration

Radiation function

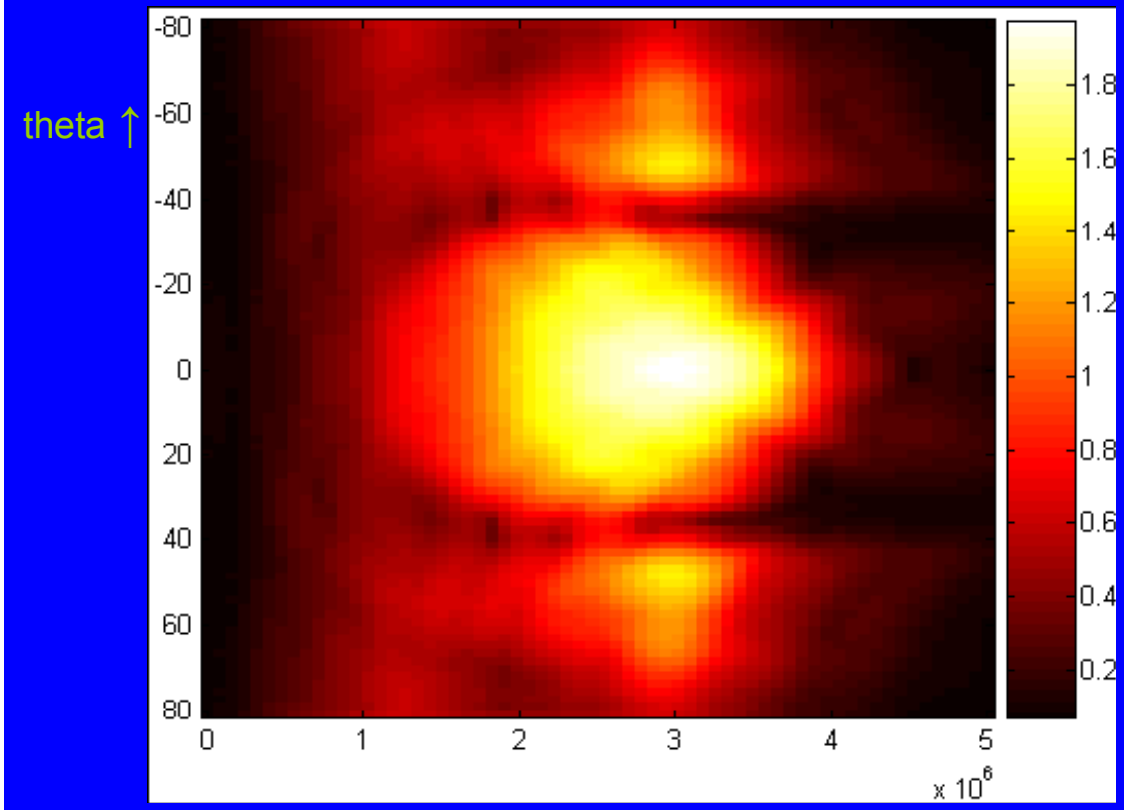

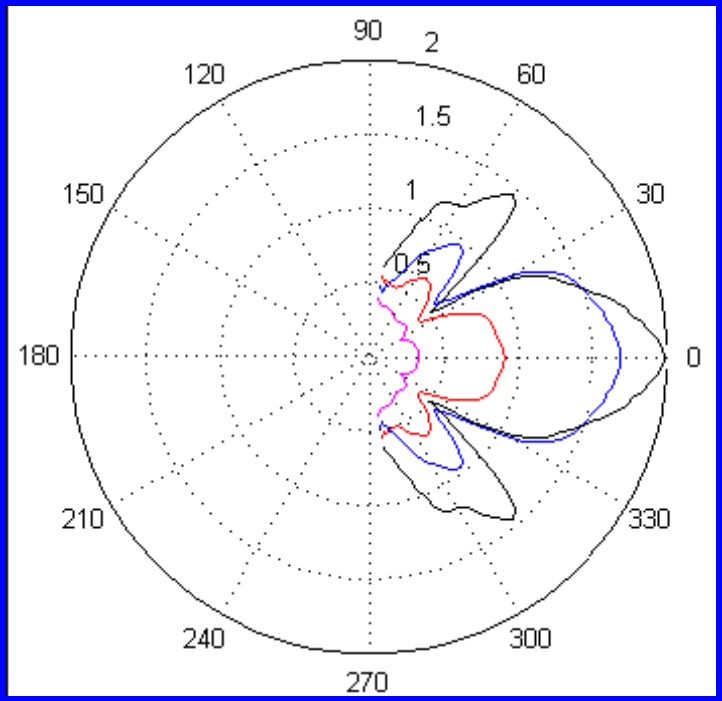

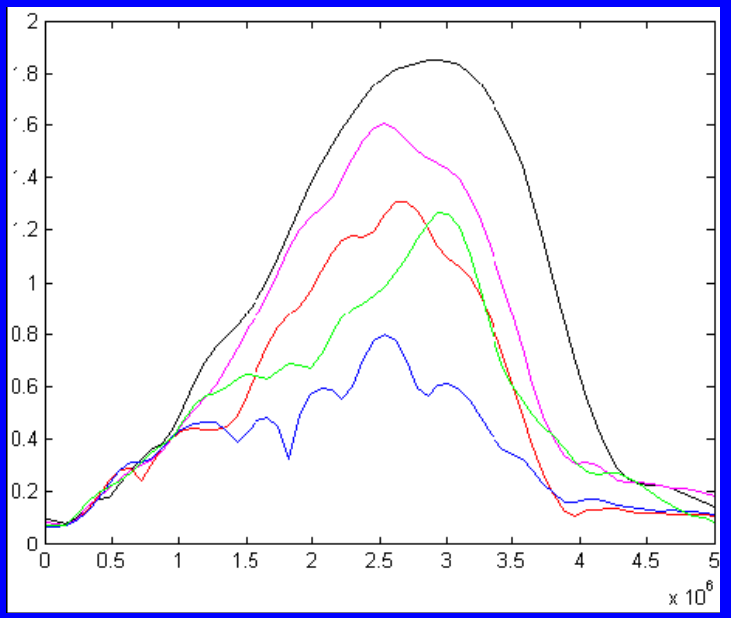

Table of transducer efficiencies

0.75 0.95 1.15 0.97 0.99 0.89 1.04

0.95 0.99 1.06 0.98 1.09 1.11 1.15

Discussion (of ultrasonic transducer field calibration)

Comparison with the experimental measurement of a transducer field via a hydrophon

(solid – acustic pressure,
dashed – calculation, co-normalized)

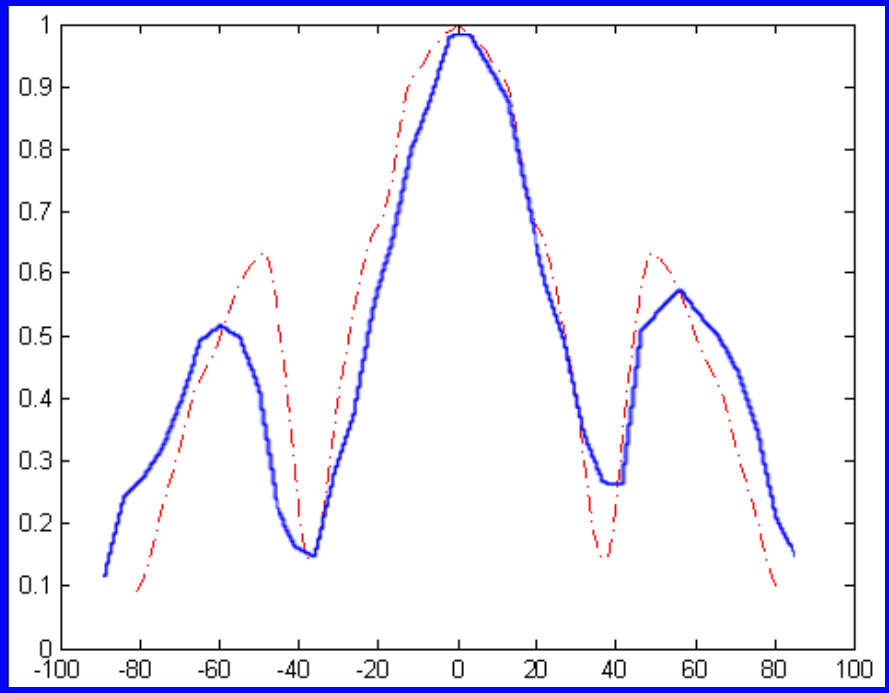

The calibration yields surprisingly consistent results.

The comparison with the measurement shows a reasonable correlation – the calibration results thus may be acceptable for reconstruction attempts.

Automated Optic Disc Segmentation in Bimodal Images of Retina

(R. Chrastek, L. Kubecka, J. Jan,
G. Michelson, V. Derhartunian, H. Niemann - Euro-DOG Congress Berlin 2005)

The project goal:

- early diagnosis of ophtalmic, cerebrovascular and other diseases (primarily glaucoma) in screening via image data analysis
- requires full automation of image analysis:
  - to prevent inter- and intra-observer variability
  - to improve sensitivity and specificity of derived diagnostic features
  - potentially to increase the patient throughput
- necessary intermediate result: automatic segmentation of the optic disc using information available in two modalities:
  - scanning-laser-tomography (SLT) image data
  - colour fundus photographic data (CFP)

Structure of the project

- pre-processing of image data in both modalities
  - noise suppression
  - non-uniform illumination correction
  - edge enhancement (in some cases)
- registration of CLT and CFP images
  - to obtain vector valued images → more reliable analysis
- optic nerve head (ONH) detection and segmentation
  - in individual modalities + merging of individually found borders
  - in the vector valued (registered) image

Preprocessing

- green channel of the CFP as approximation of PCA result is taken
- noise smoothing
- correction of non-uniform illumination (from the background illumination model approximated by median filtering with a large mask)

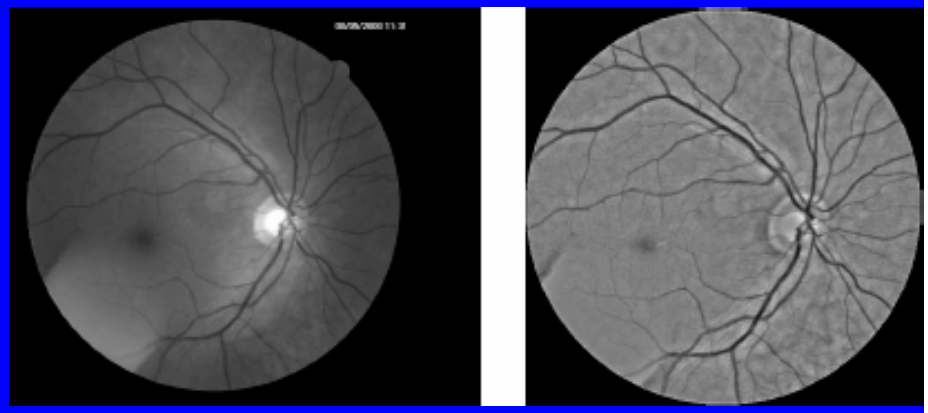

CFP image - original and corrected for nonuniform illumination (760x570, RGB 24 →8 bits, 45^0 FOV, resolution 20um/px)

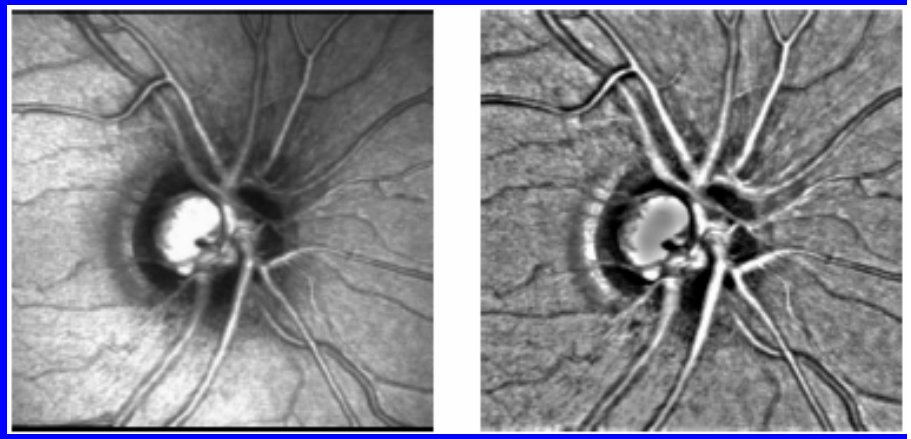

SLT reflectivity image - original and corrected for nonuniform illumination (HRT II images 384x384, 8 bits, 15^0 FOV, resolution 10um/px)

Bimodal image registration

$$\mathbf{x}_B = \mathbf{T}_\alpha \, \mathbf{x}_A$$

images to be registered:

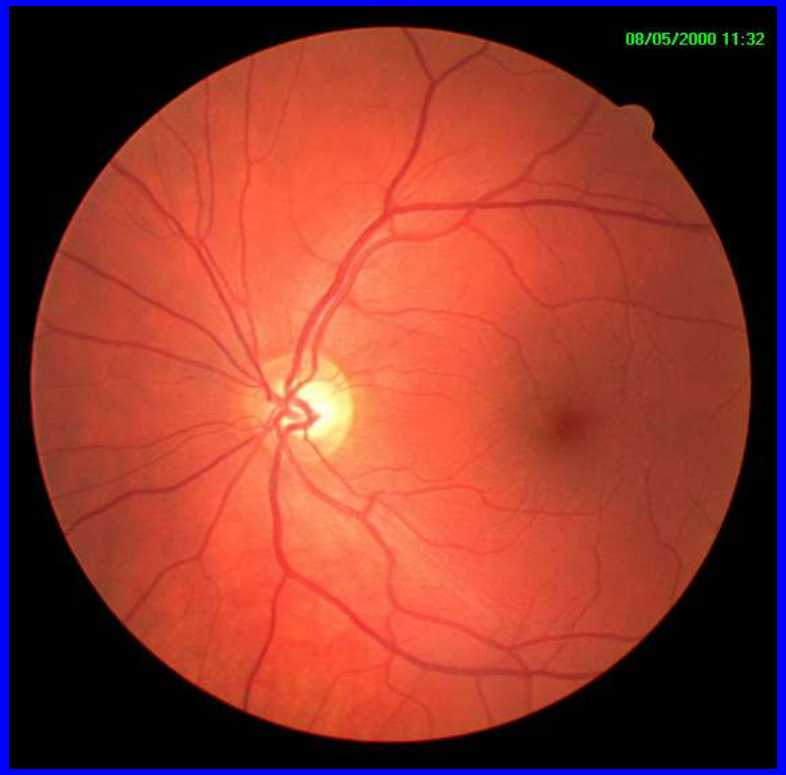

fundus camera image

(to be transformed image A)

intensity HRT image

(fixed image B)

Optimisation

$$\boldsymbol{\alpha}_0 = \arg\min_{\boldsymbol{\alpha}} \left[C\left(\mathbf{B}, \mathbf{T}_{\boldsymbol{\alpha}}(\mathbf{A})\right) \right]$$

- transform selection
  rigid transforms insufficient → affine transform

$$\mathbf{T}_{\boldsymbol{\alpha}} = \begin{bmatrix} \left(\cos(\varphi)\left(1 + g_x g_y\right) + \sin(\varphi) g_y\right) s_x & \left(\cos(\varphi) g_x + \sin(\varphi)\right) s_y & t_x \\ \left(-\sin(\varphi)\left(1 + g_x g_y\right) + \cos(\varphi) g_y\right) s_x & \left(-\sin(\varphi) g_x + \cos(\varphi)\right) s_y & t_y \\ 0 & 0 & 1 \end{bmatrix}$$

- basic similarity criterion
  incompatible contrast scales
  → **MI** criterion

$$I(\mathbf{A}, \mathbf{B}) = H(A) + H(B) - H(A, B)$$

$$= \sum_{a=1}^{m} \sum_{b=1}^{n} p(f_a, f_b) \log \frac{p(f_a, f_b)}{p(f_a) p(f_b)}$$

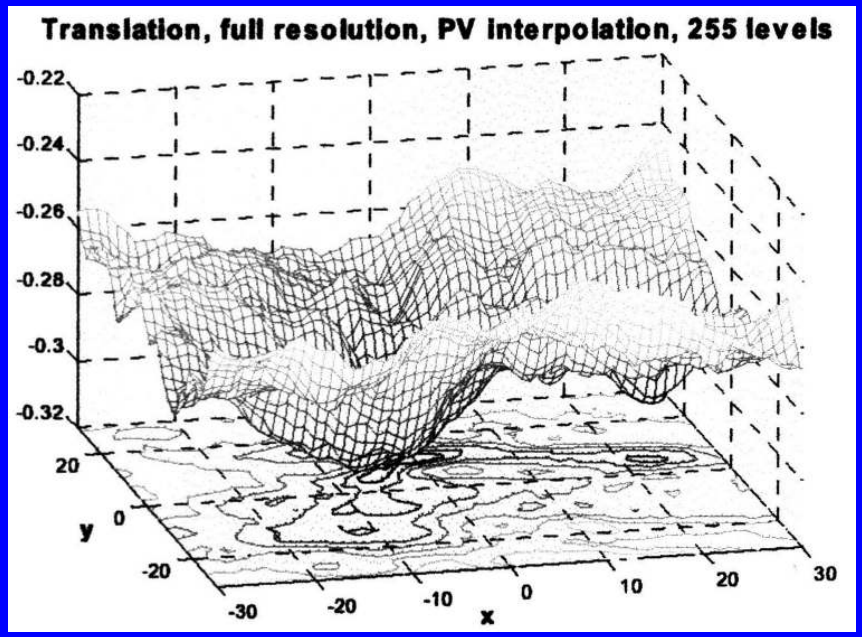

Advances in methodology

- combined registration criterion and identificaton of its properties
- change of structure of registration pyramid
- stochastic optimisation by CRS/AH method

leading to

- reliable fully automated registration
  (as opposed to previous semiautomatic approach)

combined similarity criterion

- combined criterion from MI between original images and MI of GoG images (smoothed abs-gradient)

$$C\{B, T_\alpha(A)\} = \mathrm{MI}\{B, T_\alpha(A)\} \,.\, \mathrm{MI}\{\mathrm{GoG}[B], \mathrm{GoG}[T_\alpha(A)]\}$$

- experimentally identified properties of the criterion with respect to the image type and found routinely suitable parameters:
  - Gaussian variance,
  - optimum interpolation of $T(A)$ – values (surprisingly: nearest neighbour - least artefacts in criterial values),
  - optimum image intensity resolution at ~4bits (decreasing number of bins in the joint histogram – faster and more stable computation though compromised precision)

new structure of the registration pyramid

four layer multi-resolution optimisation

level 1: 4-times subsampled
- rough global registration – translation only
- stochastic optimization routine – CRS/AH (or SA)

level 2: 4-times subsampled
- flexible global registration – affine transform
- stochastic optimization routine – CRS/AH (or SA)

level 3: 2-times subsampled
- refining the affine transform
- stochastic optimization routine – CRS/AH (or SA)

level 4: full resolution
- fine tuning of the affine transform parameters
- deterministic optimisation - simplex method

controlled random search algorithm - CRS

gradually converging contraction of a set of estimates (Price 1979)

generate population $P=\{\mathbf{x}_n\}$, i.e. N random points from the search space X
repeat
find $\mathbf{x}_{max}$ from P so that $C(\mathbf{x}_{max}) \geq C(\mathbf{x}_n)$, $\forall n$
  repeat
    $\mathbf{y} \leftarrow h(P)$, where $\boldsymbol{y}$ is from the search space.
  until $C(\mathbf{y}) < C(\mathbf{x}_{max})$
  $\mathbf{x}_{max} \leftarrow \mathbf{y}$.
until termination condition

h – a heuristics finding a new point y from the search space

CRS/AH: CRS with adaptive or alternating heuristics

Example of population sets part 1

(unions of individual sets in successive iteration steps, level 1)

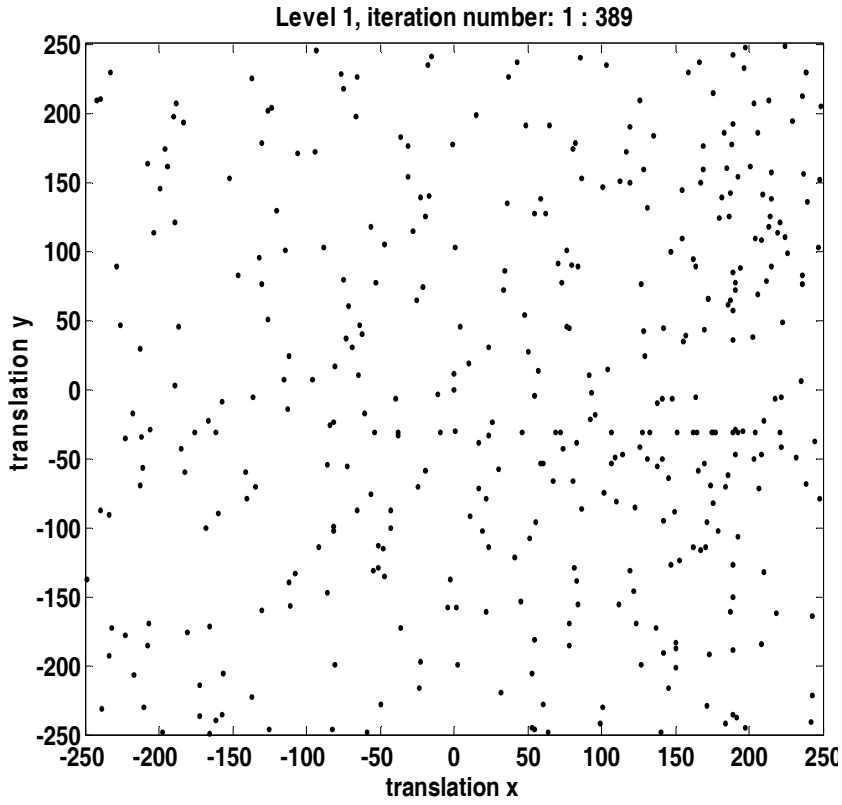

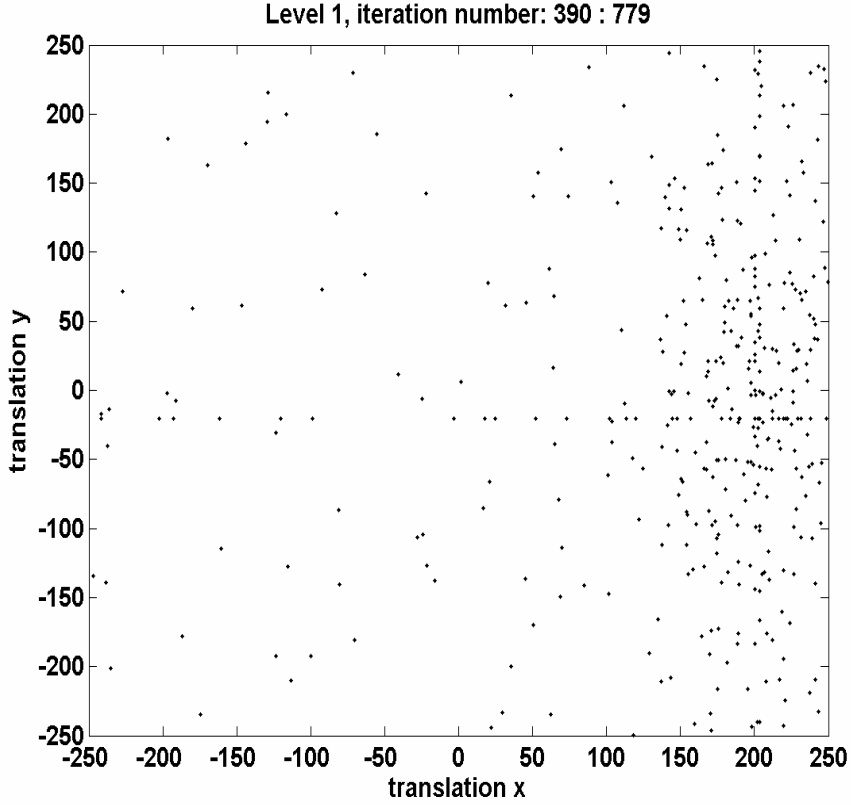

Example of population sets part 2

(unions of individual sets in successive iteration steps, level 1)

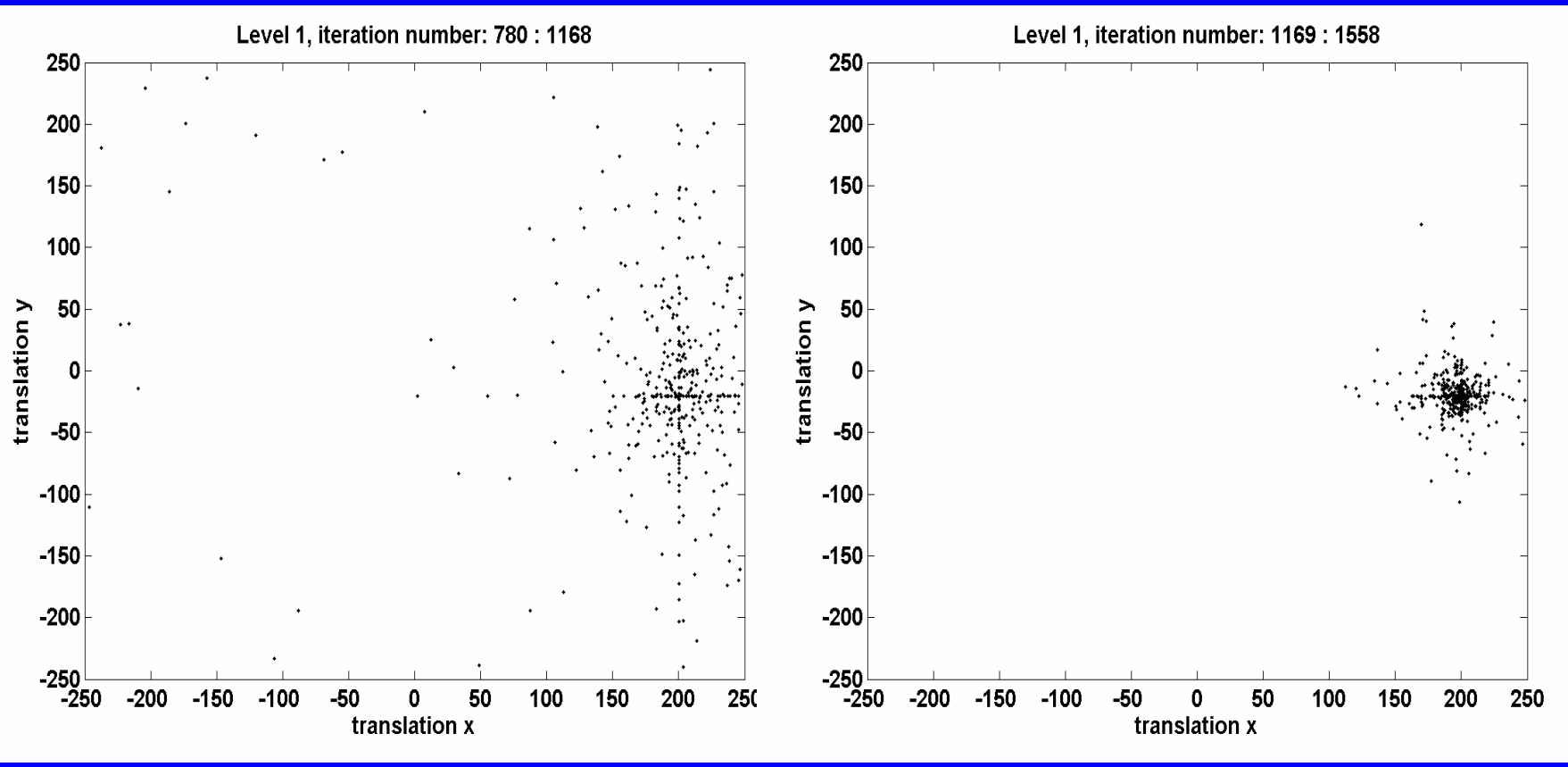

Example of population sets part 3

(unions of individual sets in successive iteration steps, level 1)

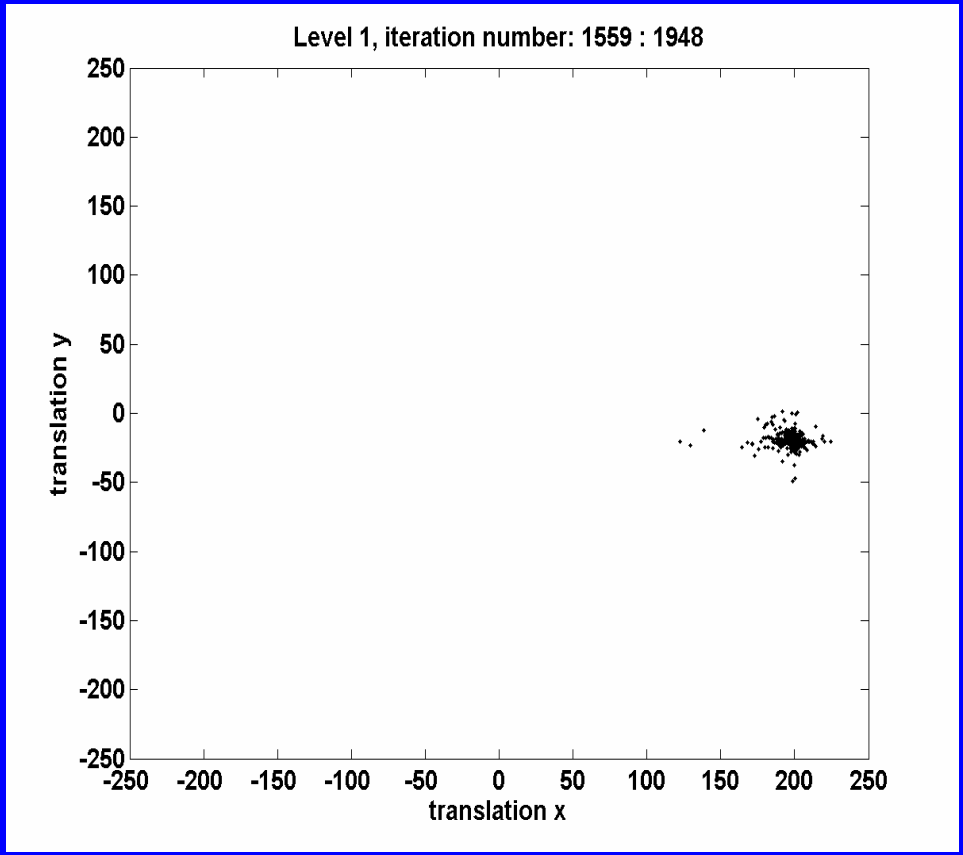

Example results

On the first level

B–image

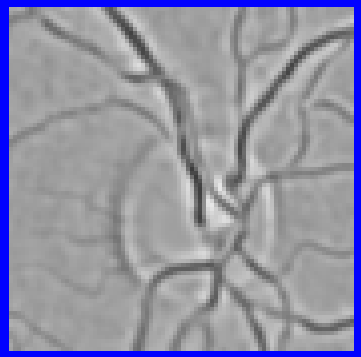

A–image registered

On the fourth level

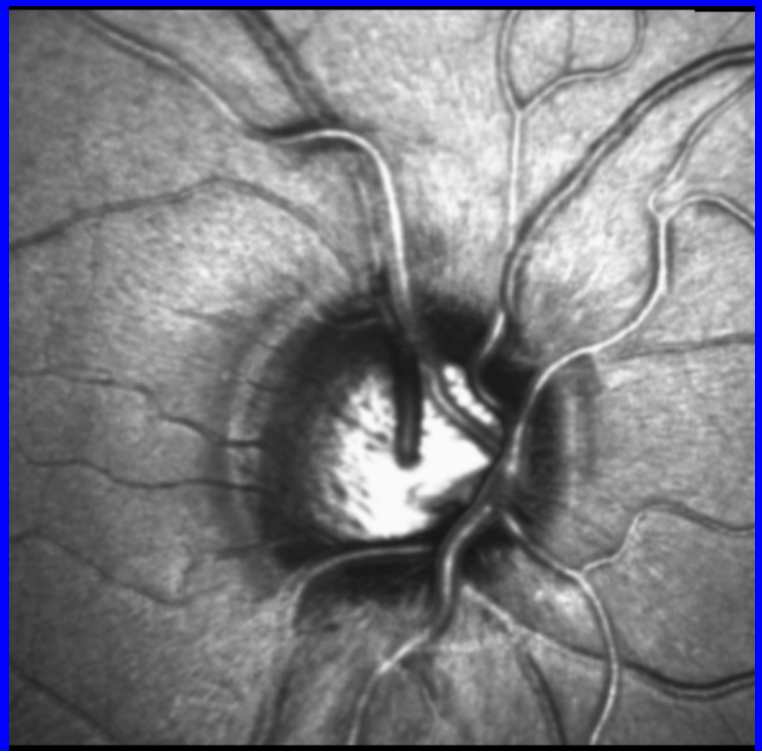

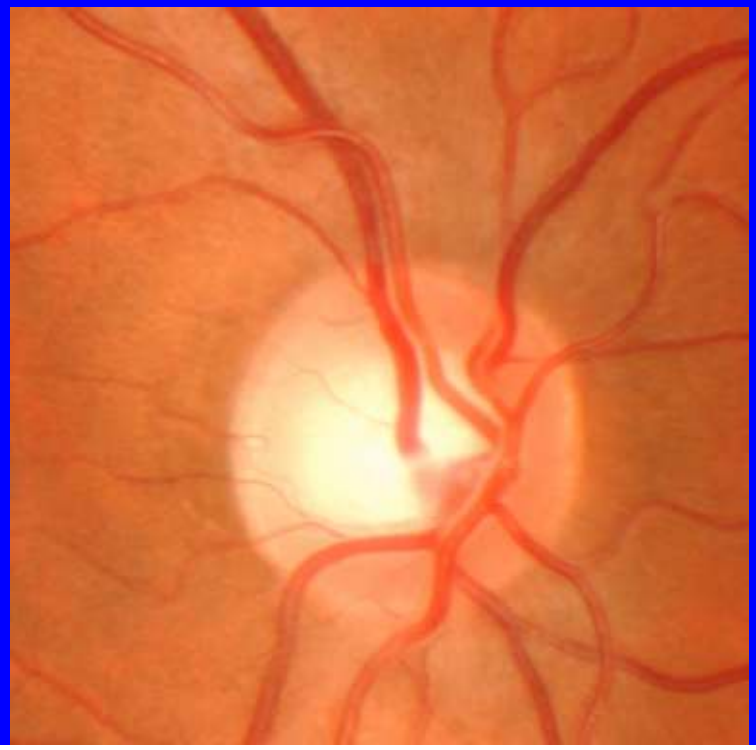

Example results

On the first level

A–image

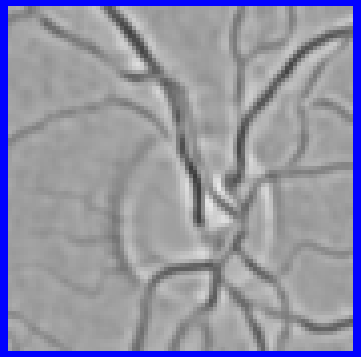

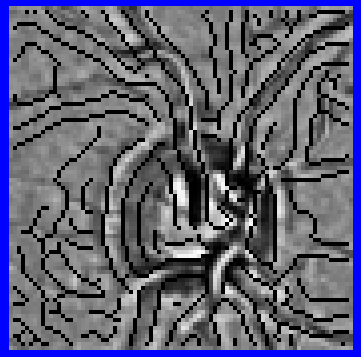

A-edges overlaid on B-im.

On the fourth level

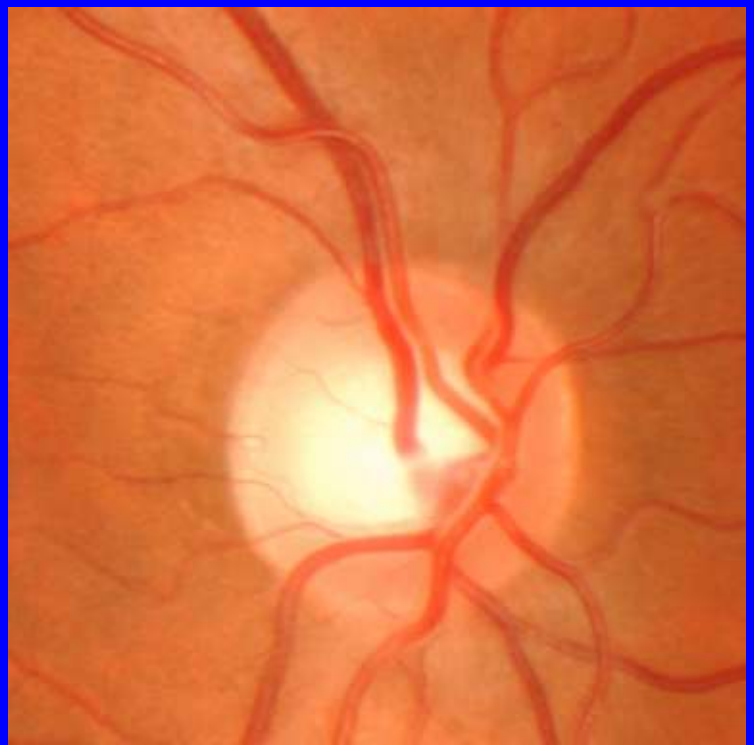

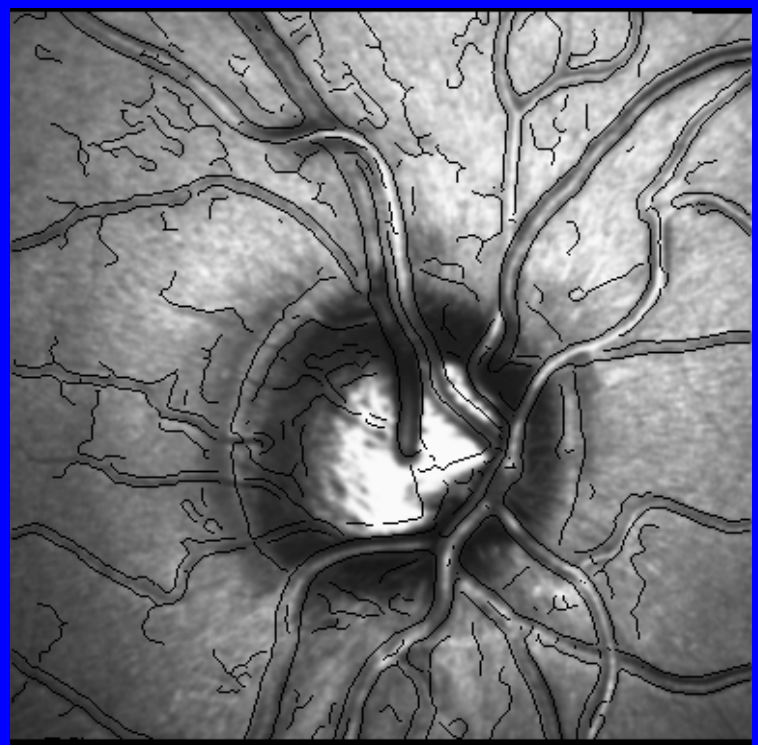

Results of statistical evaluation

Success rate of the algorithms based on CRS/AH OR SA optimisation (174 image pairs, 5 times, randomised)
Success of a pair: all 5 proper registrations

Method	***CRS/AH***	***SA***
Number of image pairs, 5-times registered	174	174
Wrong preliminary optic disc detection	4	5
Unsubstantiated misregistration	2	14
Low quality input images	4	4
Rate of success [%] (all image pairs)	94,2	86,8
Rate of success [%] (low quality images excluded)	96,5	88,8

Summary of registration phase

- combined MI-based similarity criterion ($MI \cdot MI_{GoG}$) has proved more efficient than the plain MI
- more efficient optimisation pyramid and routinely usable parameters of the algorithm found
- stochastic global optimisation based on CRS with alternating heuristics found more reliable (and less difficult to adjust) than SA, providing a high success rate up to 98%
- as a result, fully automated registration formulated, as clinically required

Segmentation Phase

present state:

- separate segmentation in individual modalities
  plus fusion of the individual results

a prospect:

- segmentation in fused (vector-valued) image
  with expected higher reliability thanks to a higher information content

Segmentation in CFP images

- applying the Hough transform to the edge representation of the image

- registered CFP (green channel) with superimposed localized position of the ONH and border of region-of-interest (ROI)

- cropped ROI

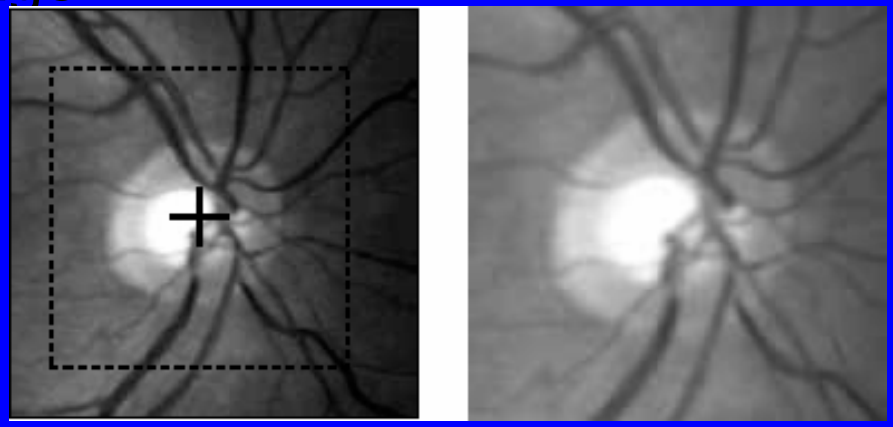

- filtered ROI

- edge image with superimposed resulting contour of the ONH

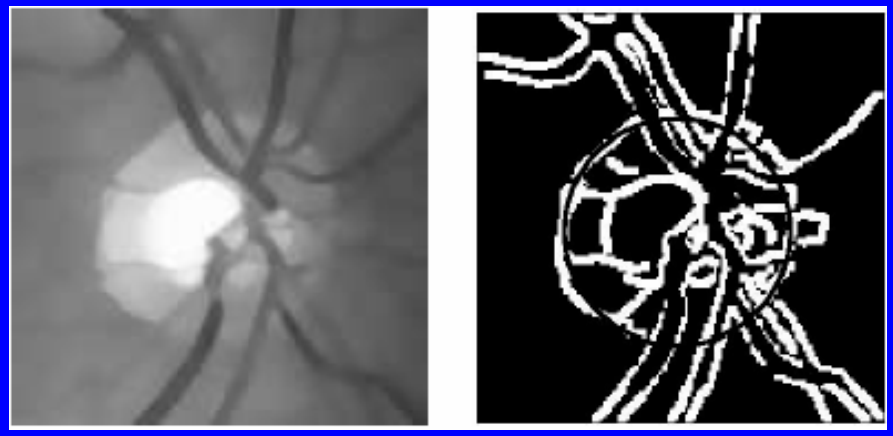

Segmentation in SLT images

- rough position of the ONH is obtained as a center of gravity of the roughly segmented neuroretinal rim (NRR)
- NRR is segmented by thresholding followed by morphological operations
- circle fitting procedure (via Hough transform)

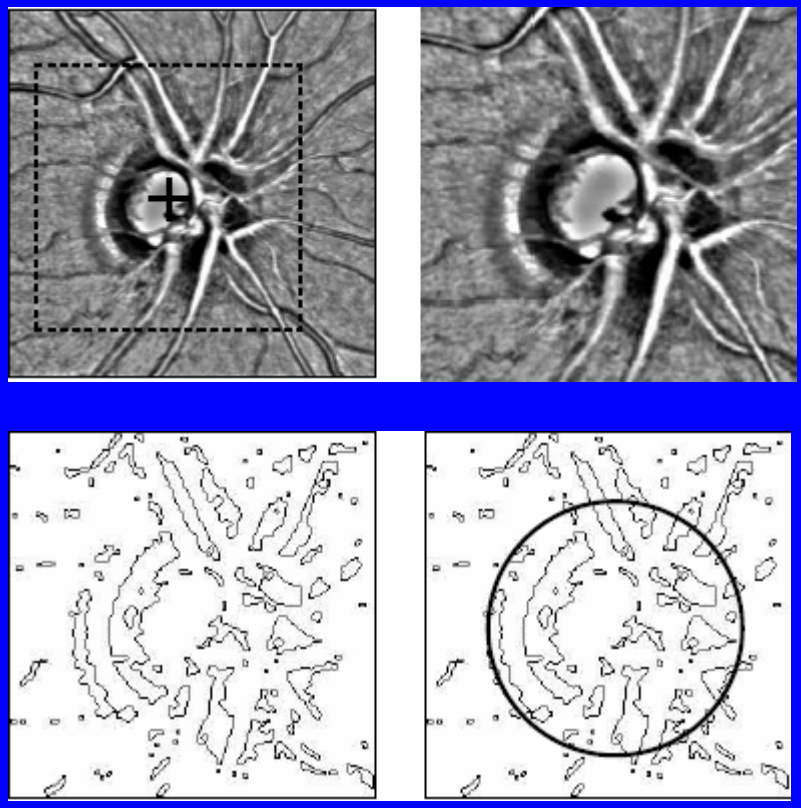

ONH localization in SLT image and approximation of the ONH by a circle:
(a) SLT reflectivity image with superimposed localized ONH position and border of ROI
(b) cropped ROI
(c) perimeters of binary image
(d) result of circle fitting.

Circle fitting via Hough transform

Purpose: constraining the search space for the potential flexible contours:

- (a) input binary image for the Hough transform to detect neuroretinal rim NRR
-
- (b) detected NRR

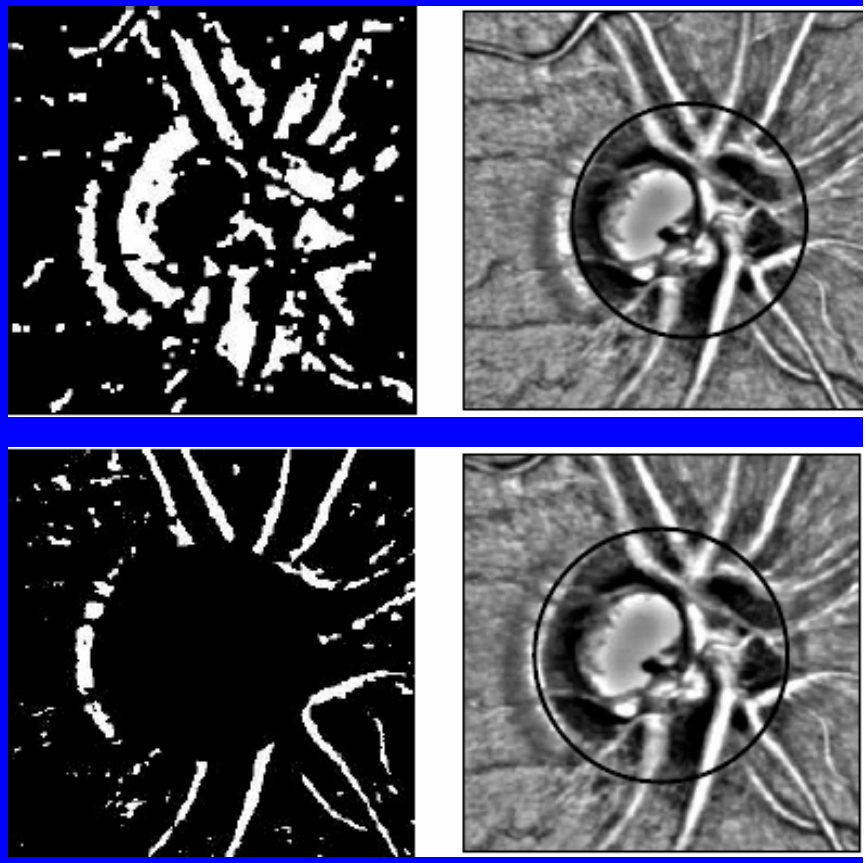

- (c) input binary image for the Hough transform for PPA detection
- (d) detected parapapillary atrophy PPA.

Fine Segmentation via Active Contours Model

- choosing optic nerve head (ONH) border from a family of controlled closed continuous splines (Active Contours)

- determination of anchors:
  - spatial constraints
  - anchor determination

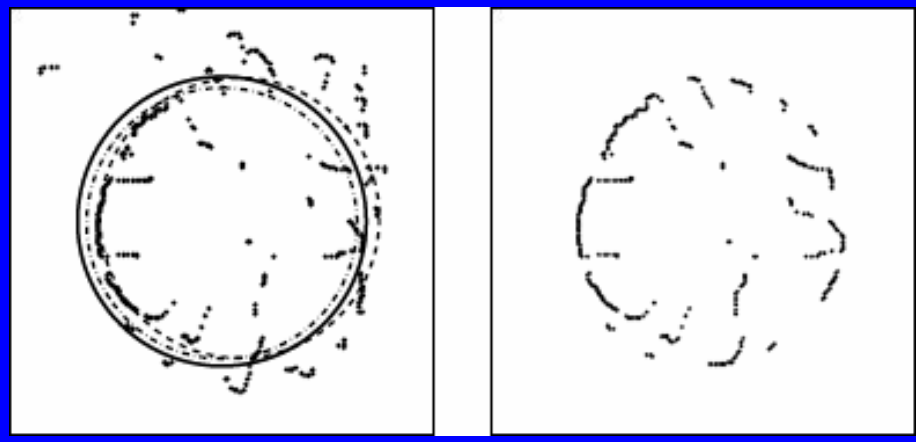

(a) The search space for anchor determination constrained by a circle approximating the ONH in CFP (solid line), the NRR (dashed line) and the PPA (dashed-dotted line)
(b) (b) anchor candidates

Flexible active contour development

Anchored active contour development:

- (a) initial curve obtained from CFP superimposed on valid anchor candidates
- (b) established spring connections between the initial curve and valid anchors

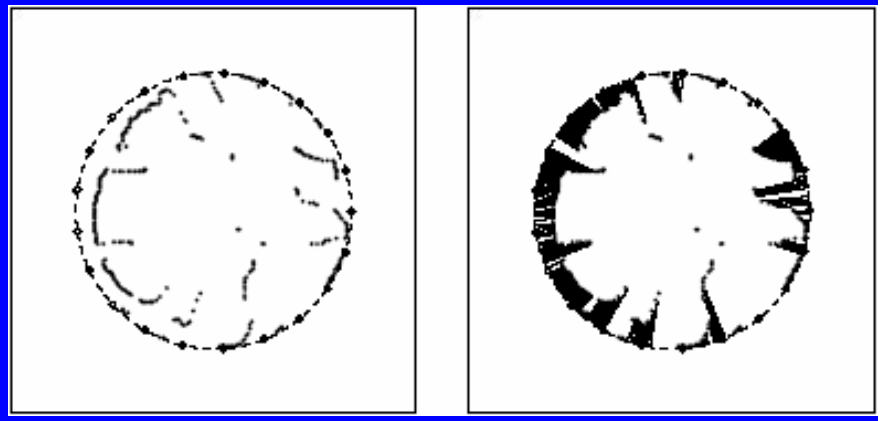

- (c) the fitted contour
- (d) the fitted contour (solid line) superimposed on the original image together with the manually marked contour (dashed line)

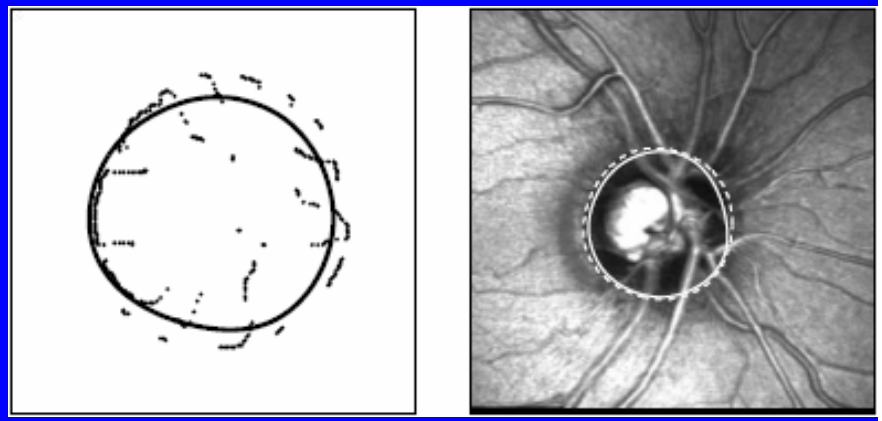

Example results

A few examples of results:

- (solid line - multimodal segmentation
- dashed line - manual segmentation
- dashed-dotted line - monomodal segmentation)

- (a)-(c) very good results with remarkable improvement

- (d) failure of bimodal segmentation

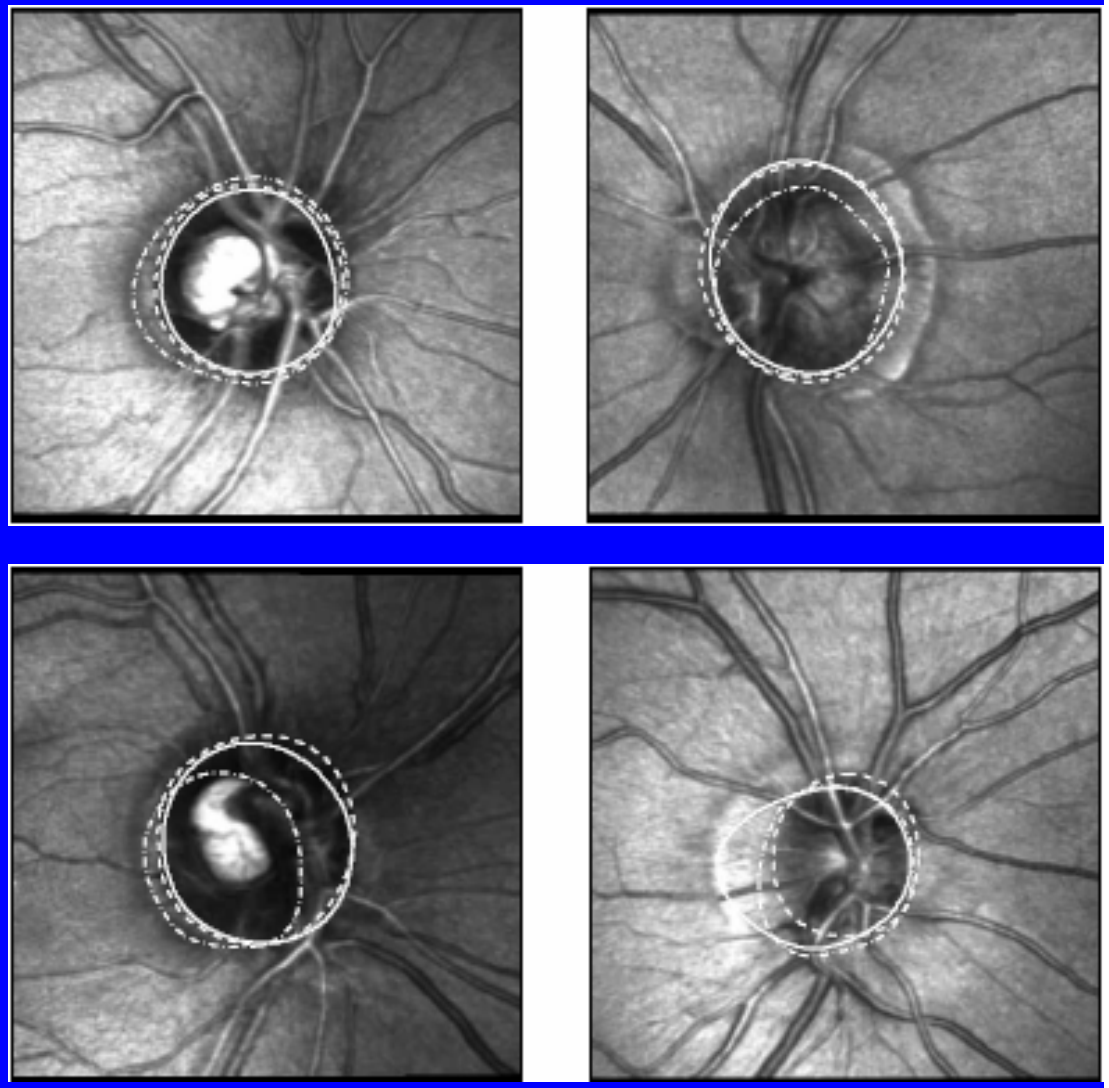

Conclusions (retinal images)

- reliable automatic approach to segmentation of the optic nerve head in the SLT images or registered bimodal retinal images
- multimodal approach is remarkably superior to monomodal segmentation
- we hope to have provided a clinically applicable tool for automated optic nerve head segmentation

Apologies to the reader:

The survey presentation was generated using several source presentations. Unfortunately, the task of combining the partial sources turned out to exceed the capabilities of the used software; consequently, the typographical appearance of the result is not as expected.